HHS Public Access

Author manuscript

Nat Chem Biol. Author manuscript; available in PMC 2015 July 01.

Published in final edited form as:

Nat Chem Biol. 2015 January ; 11(1): 38–45. doi:10.1038/nchembio.1689.

Lipid-linked cell wall precursors regulate membrane association of bacterial actin MreB

Kathrin Schirner[1], **Ye-Jin Eun**[2], **Mike Dion**[2], **Yun Luo**[3], **John D. Helmann**[3], **Ethan C. Garner**[2,*], and **Suzanne Walker**[1,*]

[1]Department of Microbiology and Immunobiology, Harvard Medical School, Boston, MA 02115, USA

[2]Department of Molecular and Cellular Biology, Harvard University, Cambridge, MA 02138, USA

[3]Department of Microbiology, Cornell University, Ithaca, NY 14853, USA

Summary

The bacterial actin homolog MreB, which is critical for rod shape determination, forms filaments that rotate around the cell width on the inner surface of the cytoplasmic membrane. What determines filament association with the membranes or with other cell wall elongation proteins is not known. Using specific chemical and genetic perturbations while following MreB filament motion, we find that MreB membrane association is an actively regulated process that depends on the presence of lipid-linked peptidoglycan precursors. When precursors are depleted, MreB filaments disassemble into the cytoplasm and peptidoglycan synthesis becomes disorganized. In cells that lack wall teichoic acids, but continue to make peptidoglycan, dynamic MreB filaments are observed, although their presence is not sufficient to establish a rod shape. We propose that the cell regulates MreB filament association with the membrane, allowing rapid and reversible inactivation of cell wall enzyme complexes in response to the inhibition of cell wall synthesis.

Keywords

MreB; Teichoic Acid; Peptidoglycan; *Bacillus subtilis*; cell envelope

Introduction

In eukaryotes, the actin cytoskeleton is required for a variety of processes, including cell shape determination, cell division and motility, wound repair, and cell signaling. The MreB

*Corresponding authors: suzanne_walker@hms.harvard.edu, egarner@fas.harvard.edu.

Author Contributions

K.S., Y-J.E., E.G., J.H. and S.W. designed the experiments; K.S. and E.G. took images for targocil treatment and TarGH depletion; Y.-J.E. and K.S. did the experiments for repletion and for imaging with various TIRF angles; M.D. provided various strains, helped with the microscopy and provided preliminary results; K.S. prepared the samples for, and Y.L. performed and analysed the microarray; other experiments and all image analysis were done by K.S.; K.S. and S.W. wrote the paper.

Competing financial interests

The authors declare no competing financial interests.

family of proteins is considered to be the prokaryotic ancestor of eukaryotic actins. MreB is conserved in most rod-shaped bacteria, and recent studies revealed that MreB proteins form short membrane-associated filaments that rotate independently around the cell width[1–6]. MreB filaments are required for cell shape determination[7,8], as cells deleted for MreB homologues become spherical,[9–11]. Current models suggest that MreB determines cell shape by positioning the biosynthetic complexes that build peptidoglycan (PG)[12–16], and a recent study shows that a complex feedback between cell geometry and MreB localization is required for rod-shape formation in *E. coli*[17].

PG is the major conserved component of the bacterial cell envelope. Composed of a polymer of glycan chains cross-linked by peptide bridges, PG forms a large sacculus around the entire cell. PG is assembled on the cell surface from a lipid-linked disaccharide precursor, lipid II, which is produced inside the cell (Fig. 1). Once formed, lipid II is flipped across the membrane and then integrated into existing PG by enzymes known as penicillin-binding proteins (PBPs). The lipid carrier for the PG precursor, undecaprenyl phosphate (UndP), is then recycled. Because the PG synthetic pathway is unique to bacteria, it is a prime target of clinical antibiotics. Many different classes of compounds inhibit various points in the biosynthetic pathway (Fig. 1), and have been useful for investigating the biology of cell wall synthesis. PG inhibitors also have an effect on MreB: It has been shown that MreB filament motion freezes immediately when PG synthesis is inhibited, suggesting that ongoing PG synthesis powers filament dynamics[1–3].

In most Gram-positive organisms, including *B. subtilis*, the cell wall contains another class of polymers called wall teichoic acids (WTAs). These polymers, which make up as much as 50% of the cell wall mass, are typically composed of linear sugar phosphate repeats (in the case of *B. subtilis*, glycerol phosphates) that are attached to the PG layer. Though it is clear that WTAs have important functions in cell growth, cell division, and the development of antibiotic resistance, their molecular functions are poorly understood. WTA precursors are synthesized on the cytoplasmic surface of the membrane attached to the same UndP carrier lipid used for PG precursors. These are then flipped across the membrane by an ABC-type transporter, TagGH, and attached to PG (Fig. 1). The first genes in the pathway (*tagO/A*) can be deleted, showing that *B. subtilis* cells lacking WTAs are viable, but they lose their rod shape[18,19]. However, blocking the WTA biosynthetic pathway after the early steps prevents cell growth as the essential carrier lipid (UndP) becomes trapped in an intermediate[20], depriving the cell of the ability to make PG. It has been observed that several enzymes involved in WTA synthesis may interact with MreB[21], as their localization changes on MreB depletion, but it is not known how activity of these enzymes affects the motion of MreB filaments.

Here we show that in *B. subtilis* MreB still forms dynamic filaments in a *tagO* deletion strain lacking WTAs, demonstrating that the presence of WTA polymers is not required for MreB filament motion. Blocking a late step in the WTA pathway however results in MreB filaments dissociating from the membrane into the cytoplasm. We show that multiple small molecule inhibitors or genetic constructs that deplete the PG intermediate lipid II have the same effect on MreB, and conclude that membrane association of MreB depends on an adequate supply of membrane-bound PG precursors. Hence, we propose that the assembly

of cell wall synthetic complexes, which depend on MreB filaments, are mediated by the cellular levels of the PG precursor lipid II.

Results

Inhibiting WTA export causes MreB filaments to dissolve

To probe the effect of inhibiting WTA synthesis on MreB motion, we took advantage of the small molecule targocil, a late-stage WTA inhibitor that inhibits growth of *S. aureus* by blocking the WTA exporter TarGH (Fig. 1)[22,23]. *B. subtilis* can be sensitized to targocil by replacing the *B. subtilis* WTA exporter with *S. aureus* TarGH[24], making it possible to study how WTA inhibition affects MreB dynamics.

We visualized MreB dynamics during WTA inhibition using live-cell microscopy. A targocil-sensitive strain expressing MreB-GFP (EG133) was grown on a microscope slide, and targocil was added during the acquisition of a time-lapse series, imaging every 30 sec over 30 min. Although targocil depletes lipid II[20] its addition did not halt MreB motion as PG synthesis inhibitors did[1,2]. Rather, motion slowed and MreB filaments gradually dissolved, resulting in a diffuse fluorescent signal (Fig. 2a and b, Supplementary Movie 1). Targocil does not have any secondary targets in *B. subtilis*[24] and had no effect on cell growth or MreB-GFP motion in cells with wild type WTA transporters (Supplementary Results, Supplementary Fig. 1a, b, Supplementary Movie 2). Therefore, the observed effect is due to inhibition of WTA synthesis. Consistent with this, genetic depletion of TarGH, the molecular target of targocil, resulted in the same phenotype: after 2 h depletion, visible MreB foci had completely dissolved (Supplementary Fig. 1c, Supplementary Movie 3). The disassembly of MreB is not due to cell death because after 1 h of treatment the majority of cells were still viable; indeed, cells continued to grow at this time point (Supplementary Fig. 1d, e). Importantly, the dissociation of MreB filaments is a reversible process: cells with diffuse MreB recovered membrane-associated dynamic filaments within 10 minutes after targocil was washed out (Fig. 2c, Supplementary Movie 1).

Mislocalized PG synthesis during WTA synthesis inhibition

MreB has been proposed to organize the cell wall synthetic complexes. Thus, we tested whether the motion of PG synthetic enzymes was affected when MreB was depolymerized. Pbp2A, the MreB-associated transpeptidase, has a population of molecules that move directionally around the cell at the same rate and angle as MreB[1]. To analyze Pbp2A motion, we quantitated several metrics from our data, diagrammed in the schematic of Fig. 3a. Panel I shows a schematic of an image taken at a single time point, illustrating the expected spotty pattern of fluorescence. Panel II shows the result of superimposing all individual snapshots within a series results to a maximum intensity projection, which provides information about protein location over the entire time interval; for directionally moving particles this results in a series of bands. Panel III shows kymographs generated perpendicular to the long axis, which give information about protein motion: circumferential, directional motion results in diagonal lines. Panel IV shows measurements of the fluorescence intensity at the center of a kymograph along the time axis, representing the temporal changes in fluorescence intensity at one spot in the cell. For example, under normal growth conditions Pbp2A-GFP gives a

hill-and-valley pattern as the signal appears and disappears regularly over time. Finally, we analyzed the variance of the fluorescence intensity over the entire field in respect to time (Fig. 3a, V). This analysis reflects the variance in fluorescence intensity at each pixel over the whole time lapse. Red indicates areas of high variance, showing dynamic protein complexes with resolvable motion, and blue indicates areas of low variance, in which there is no directed resolvable motion. These analyses were performed for all time lapses reported below, and are included in the supplementary information.

We constructed a fluorescent fusion of Pbp2A at its native locus and promoter (strain bMD99), acquiring time lapse movies (1 sec intervals, 100 sec total). In untreated cells, we observed small patches of GFP-Pbp2A moving around the width of a cell, as previously reported (Fig. 3a, Supplementary Movie 4). After cells were treated with targocil for one hour, the directed motion disappeared and the signal stayed constant over time with the exception of photobleaching (Fig. 3a, Supplementary Movie 4). Kymographs and temporal variance analysis confirmed that directional motion of Pbp2A was abolished after targocil treatment (Fig. 3a, panels III–V). Considering that targocil treatment eventually inhibits lipid II synthesis[20], this observation is consistent with a previous study using a nisin variant as a specific lipid II inhibitor, which also reported the mislocalization of PBPs in treated cells[25].

We next visualized nascent PG synthesis using a fluorescently tagged D-amino acid, HADA (hydroxycoumarin-carbonyl-amino-D-alanine), which is actively incorporated into PG by cell wall synthetic enzymes[26,27]. After pulse labeling, untreated cells showed a regular “banded” pattern of PG synthesis over the cylindrical part of the cell as well as strong septal labeling at mid-cell (Fig. 3b, Supplementary Figure 2a)[26]. In targocil-treated cells the pattern of labeling dramatically changed: instead of a lateral even staining and strict mid-cell distribution, bright foci were observed that were still often located at mid-cell or cell poles, but also found randomly located throughout cells. Importantly, the lateral labeling was largely absent (Fig. 3b, Supplementary Figure 2a, c).

Similar results were observed using fluorescent vancomycin (VanFL), which binds noncovalently to nascent (uncrosslinked) PG on the cell surface. Untreated cells showed an even pattern of labeling along the side walls and septa, while in targocil-treated cells signal was only observed in patches close to mid cell but was absent laterally (Fig. 3b, Supplementary Figure 2b, c). Combined, these results show that lateral PG synthesis is absent when WTA synthesis is blocked and MreB filaments dissolve.

WTAs are not required for MreB filament formation

We considered several hypotheses for why MreB filaments disassemble when WTA biosynthesis is inhibited at a late step. The accumulated WTA precursor molecules in the cytoplasm might inhibit MreB filament localization, or WTA on the outside of the cell might be required for MreB filament formation. Another possibility is that MreB filaments might be regulated by cell wall stress response pathways. Alternatively, MreB filament localization might depend on the presence of undecaprenyl phosphate (UndP) or UndP-containing PG precursors, which become depleted as the carrier lipid is sequestered in WTA intermediates.

To test these possibilities, we imaged MreB dynamics in a set of mutant strains, analyzing the data as described above. To examine if the intracellular accumulation of WTA polymers affected MreB localization, we created strains with inducible control of enzymes in the WTA pathway and then introducing the MreB-GFP fusion. We first observed the motion of GFP-MreB in an inducible TagF strain. Depletion of TagF depletes WTA from the cell surface, while preventing formation of the intracellular WTA polymer; UndP remains sequestered in the non-polymeric TagB product (Fig. 4a, Supplementary Fig. 3a). During induction of TagF expression, MreB motion appeared normal. After depleting TagF for 2 h, MreB dissolved: spotty fluorescence was no longer seen in the snapshot, and the intensity variance over time was very low (Fig. 4a, Supplementary Movie 5, Supplementary Fig. 3a). These results showed a loss of MreB-GFP membrane association and dynamics after TagF depletion. Therefore, disassembly of MreB is not due to accumulation of WTA polymers inside the cell.

We next examined whether the presence of WTA on the cell surface was required for MreB motion by imaging MreB-GFP in a strain where WTA is completely absent (*tagO* deletion). TagO is the first enzyme in the WTA synthesis pathway and cells remain viable in its absence, but lose their rod shape[19,30]. Fluorescent images and analysis clearly showed that MreB filament formation and directional motion were preserved in the *tagO* deletion strain (Fig. 4b, Supplementary Movie 6, Supplementary Fig. 3b). Therefore, WTA itself is not required for MreB filament formation or directional motion. This also demonstrates that the presence of directionally moving MreB filaments is not sufficient for rod shape formation.

Lack of carrier lipid leads to MreB filament disassembly

We next tested the possibility that MreB filaments disassemble upon targocil treatment because blocking WTA export leads to a sequestration of the undecaprenyl carrier lipid (UndP), required for both PG and WTA synthesis[20]. If this were the case, a genetic depletion of UppS, the protein responsible for the synthesis of undecaprenyl pyrophosphate (UndPP), should have the same effect. We constructed a strain with *uppS* under the control of an inducible promoter and imaged MreB-GFP while depleting UppS. After 4 hours of depletion, the time span necessary to deplete UppS in this strain MreB-GFP dissolved (Fig. 4c, Supplementary Movie 7, Supplementary Fig. 3c, d), similar to the targocil treated or TagF depletion strains. This phenotype was not due to cell death: at this time point depleted cells were still viable and able to form colonies (Supplementary Fig. 3e). Taken together, this data suggested that depolymerization of MreB was most likely caused by depletion of either UndP itself or an UndP-containing cell wall precursor.

Only cell wall inhibitors lead to MreB disassembly

While PG synthesis inhibitors have diverse mechanisms of action, all eventually lead to depletion of intracellular UndP-linked precursors. Therefore, if depletion of UndP-linked PG precursors causes MreB to dissolve, one would expect PG synthesis inhibitors to have the same effect. In previous work demonstrating that MreB motion freezes after the addition of PG synthesis inhibitors[1–3], cells were studied for only a few minutes, a time scale too short for cells to deplete available carrier lipids. We tested a panel of inhibitors with different targets in the PG synthetic pathway (Fig. 1). After treatment times corresponding to 1–2

generations (1 h), vancomycin, tunicamycin, fosfomycin, ampicillin, and bacitracin all caused MreB filaments to dissolve (Fig. 5a, Supplementary Fig. 4, Supplementary Movies 8, 9). At this timepoint, cell growth had not ceased yet, as measured by optical density (Supplementary Fig. 5a). To ensure that MreB filament dissolution was not an artifact of overexpression, misregulation, or nonfunctional fusion proteins, we also tested strains carrying MreB and Mbl (another *B. subtilis* actin homolog) as GFP-fusions at their native loci under control of their native promoters. In both strains, treatment with vancomycin for one hour resulted in the same phenotype of dissolved MreB/Mbl (Supplementary Fig. 5b, Supplementary movies 10, 11). We also examined the effects of vancomycin, as a representative PG synthesis inhibitor, on cell viability and MreB-GFP protein levels. 1 h after vancomycin treatment, the majority of cells were still viable and the cellular MreB-GFP level was unchanged. Hence, the absence of MreB polymers was not due to cell death or protein degradation (Supplementary Fig. 6a, b). Moreover, MreB motion resumed upon removal of PG synthesis inhibitors, such as bacitracin, similar to the recovery of MreB dynamics after washing out targocil (Supplementary Fig. 6c, Supplementary Movie 12). In contrast, treatment with two protein biosynthesis inhibitors, tetracycline and chloramphenicol, had no effect on MreB filament formation and dynamics even after 1 h (Fig. 5a, Supplementary Fig. 4, movies 8, 9). Notably, cell wall synthesis was ongoing in cells treated with protein synthesis inhibitors: the labeling pattern of nascent PG with fluorescent vancomycin was indistinguishable from untreated cells, with clear labeling at the lateral and septal cell periphery (Supplementary Fig. 6d). Consistently, treatment with chloramphenicol does not render cells insensitive to antibiotic activity of a β-lactam (Supplementary Fig. 6e). Hence, at the antibiotic concentrations used, depolymerization of MreB is not a general response to growth inhibition, but is specific to cell wall synthesis inhibition. While WTA and PG synthesis inhibitors had different short-term effects, the long-term effects were identical: the MreB filaments disassemble in a reversible manner.

Non-filamentous MreB becomes cytoplasmic

MreB filaments purified from *Escherichia coli* and *Thermotoga maritima* have been shown to bind directly to membranes. Most Gram-positives, including *B. subtilis*, lack the N-terminal amphipathic helix used for membrane insertion in *E. coli* MreB, retaining only a putative membrane insertion loop[5]. We therefore wondered if MreB filaments depolymerize into the cytoplasm, or if the depolymerized MreB remains membrane-associated. To visualize this transient state in live cells, we took advantage of total internal reflection fluorescence (TIRF) microscopy[31], which gives illumination only ~200 nm from the coverslip, so that only the signal close to the membrane is visible. By increasing the angle of the incidence beyond the critical point, we illuminated the whole cell to image the cytoplasm (Supplementary Fig. 7).

We calibrated this approach by imaging cells stained with the membrane dye FM4-64. By adjusting the TIRF angle and focal plane we were able to visualize either only the cell surface in contact with the coverslip (magenta) or the mid-cell portion of the cell (green) (Fig. 5b, top). In untreated cells MreB can be seen at the convex cell surface when imaged using TIRF (magenta), and at the sides of a cell in a mid-cell angle (green), consistent with its localization to the cytoplasmic membrane (Fig. 5b, middle). As MreB filaments

disassembled under many conditions tested above, and cells appeared similar under all conditions that inhibited cell wall synthesis, we used vancomycin as our representative inhibitor. After 1 h treatment, the TIRF MreB-GFP signal at the membrane became very low (magenta), while the mid-cell focal position became bright and even throughout the cell (green) (Fig. 5b, bottom). We measured the fluorescence intensity perpendicular to the long cell axis of each cell, both in the TIRF image and the mid-cell focus image (Fig. 5c). For the membrane dye, we observe an even fluorescent signal in the TIRF image, with two clear maxima on each side of the cell in the mid-cell focus image, corresponding to the two sides of the cell (Fig. 5c, top, arrows). The two maxima are also visible in the MreB signal in untreated cells (Fig. 5c, middle), and both in the TIRF and the mid-cell focus images there is a higher variability in fluorescence patterns, because the MreB foci are not evenly distributed. In contrast, after treatment with vancomycin, the fluorescence intensities are even again, showing a uniform MreB distribution (Fig. 5c, bottom). The humps are absent, and the maximum fluorescence intensity is now in the middle of the cell, supporting the loss of MreB membrane association when cell wall synthesis is inhibited.

ECF sigma factors are not required for MreB disassembly

Cell wall inhibition induces a common set of stress response pathways. We postulated that these pathways might be the cause of MreB depolymerization. Indeed, transcriptomic analysis of *B. subtilis* treated with targocil showed that the main regulons responding to treatment are controlled by the known cell wall stress responsive ECF-type alternative sigma factors SigM and SigW, and the transcription factor Spx, itself a member of the SigM and SigW regulons (Fig. 6a)[32,33]. The activation of cell wall stress responses has been connected to changes in carrier lipid metabolism, in particular, SigM induction has been linked to depletion of UndP[32,34–37]. Therefore, we tested if any of the ECF sigma factor regulons was responsible for the dissolution of MreB by introducing MreB-GFP into a strain lacking all seven known ECF-sigma factors[38]. We observed that MreB still dissolved in this strain after 1 h of vancomycin treatment (Fig. 6b, Supplementary Fig. 8a, Supplementary Movie 13). Therefore, while we cannot exclude the involvement of other factors, MreB depolymerization occurs independently from cell wall stress responses via alternative ECF-sigma factors.

Lipid II is implicated in MreB membrane association

Our results thus far suggested that MreB membrane association in *B. subtilis* depends on the presence of an UndP-linked PG precursor, of which there are two: lipid I, the MraY product, and lipid II, the MurG product (Fig. 1). Because there are no robust methods for directly measuring these precursors in *B. subtilis*, we tested which precursor could control MreB membrane association by imaging MreB-GFP in a strain with MurG under control of an inducible promoter. Removal of inducer depletes MurG and therefore also lipid II, but lipid I is still made, although the extent to which it accumulates is limited by the reversibility of the MraY reaction. In the presence of inducer MreB filament formation and dynamics were the same as in a wild-type background, but after 4 h of MurG depletion membrane-bound MreB had fully dissolved into the cytoplasm (Fig. 6c, Supplementary Fig. 8b, Supplementary Movie 14). Reinduction of MurG expression resulted in MreB filaments reforming on the membrane and directionally moving (Fig. 6c, Supplementary Fig. 8b, Supplementary Movie

14). This revival of membrane-associated MreB filament motion occurred within 15 min of inducer addition, in some cells reaching wild-type levels within 45 min. Taken together, our data suggest that the membrane association of MreB filaments is an actively regulated process that depends on the availability of the cell wall precursor molecule lipid II.

Discussion

While MreB has been shown to be required for the coordination of the enzymes responsible for rod shape determination, the molecular mechanism by which it functions is unclear. Using specific small molecule inhibitors and genetics, we show that MreB membrane association depends on the presence of UndP-linked PG precursors. Our results lead us to propose that MreB binds either directly or indirectly to intracellular lipid II. MreB membrane association then enables filament formation and assembly of the complexes containing all enzymes required for cell elongation (Fig. 6d, top). When lipid II levels are depleted, MreB filaments disassemble into the cytoplasm and the cell wall enzyme complexes dissociate, resulting in a cessation of cell elongation (Fig. 6d, bottom). Consistent with our model, it was recently reported that *B. subtilis* MreB is linked to membrane regions with high fluidity, and it is also known that lipid II has a strong preference for such membrane regions[28,29,39].

Interestingly, eukaryotic actin has also been observed to redistribute in response to cell wall stress: underlining the resemblance to the prokaryotic homolog MreB, when cell wall integrity is perturbed in *Saccharomyces cerevisiae*, polymeric actin concentrated in the bud delocalizes over the entire cell membrane. This leads to mislocalization of cell wall synthetic proteins, which interrupts the budding process. Actin repolarizes upon relief of the stressor, enabling cells to rapidly resume growth[40].

In *B. subtilis*, several lines of evidence support the model that the cell wall precursor lipid II is required for MreB membrane localization and filament formation. All depletions or small molecule inhibitors that result in loss of MreB membrane association have in common the lack of lipid II. The WTA inhibitor targocil blocks export of the WTA precursor and leads to cell death by sequestration of the carrier lipid[20,22]. Vancomycin binds to the stem peptide of lipid II and nascent PG on the extracytoplasmic surface of the cell, which interrupts UndP recycling[41]. Bacitracin also inhibits recycling of the carrier lipid by forming a calcium complex with UndPP on the cell surface. Ampicillin blocks PG crosslinking by inactivating PBPs, which leads to decreased pool levels of intracellular PG precursors[42,43]. Fosfomycin and high concentrations of tunicamycin directly inhibit formation of lipid II by blocking upstream steps in the pathway[44,45] (Fig. 1). Under small molecule treatment the disassembly of MreB filaments began within 10 min, but took 1–2 generations to complete. Disassembly was reversible on a similar time scale. These observations suggest that MreB filament disassembly is likely due to depletion of an essential component over time, rather than a direct effect.

Linking MreB membrane association to PG precursor levels would provide a mechanism to regulate the formation of cell wall enzyme complexes (Fig. 6d). The dissociation of cell wall synthetic complexes in response to low cell wall precursor levels may ensure that the lytic

reactions stop when no PG precursors are available. *B. subtilis* MreB homologs have been connected to the formation of complexes containing both synthetic and hydrolytic enzymes[12,13,46]. The dissociation of cell wall synthetic complexes may insure that lytic reactions stop when no PG precursors are available for synthetic reactions. In support of this, we have shown that disassembly of the MreB filaments in *B. subtilis* also leads to mislocalization of cell wall synthetic complexes containing Pbp2A; moreover, lateral wall synthesis disappears. We hypothesize that coupling cell elongation to the availability of cell wall precursors through MreB filament membrane association may provide two advantages. First, this could give the cell a mechanism linking the metabolic state of the cell to its rate of growth, Second, cells can depolymerize MreB in response to stresses to halt PG synthesis, both protecting the cell and allowing cell growth to resume immediately when the stress is relieved.

Methods

Growth conditions and antibiotics

Strains were grown in LB or CH[47] medium at 37°C. Antibiotics were used at the following concentrations: vancomycin 2μg/ml, targocil 20μM, bacitracin 100μg/ml, tunicamycin 5μg/ml, ampicillin 40μg/ml, fosfomycin 10μg/ml, chloramphenicol 10μg/ml, tetracycline 10μg/ml, spectinomycin 100 μg/ml. All antibiotics except targocil are commercially available. Targocil was synthesized to order as described by Lee[23] by SRI International. To express TarGH from *S. aureus* in targocil sensitive strains, IPTG was added to the culture at 1 mM. Expression of fluorescently tagged MreB was driven by addition of 20 mM xylose or 0.2 mM IPTG as required. The TagF depletion strain was maintained in the presence of 1% (67 mM) xylose, and the UppS depletion strain in the presence of 0.2% xylose (13 mM).

Microscopy

For TIRF and Spinning disk confocal microscopy, strains were grown in CH medium at 37°C, using a shaking water bath or roller with proper aeration (1/10 liquid to air). If not indicated otherwise, antibiotics were added at above-MIC levels when cells reached exponential growth phase and incubated for an additional hour at 37°C. Then 1 ml of culture was centrifuged for 2 min at 8000 g and the pellet was resuspended in approx. 30 μl of medium. 2 μl of the resuspension were placed on a coverslip, covered with a pad of 2% agarose in CH medium containing the relevant antibiotic, and imaged at room temperature. Time lapses were taken by imaging every 30 sec over 30 min (for Fig. 2), by streaming acquisition every second over a time span of 100 seconds (for Fig. 3), or every 10 sec over 5 min (Fig. 4–6). For Fig. 2, targocil was added to the cells under the microscope after frame 3 (1 min) of the time lapse (12 μl of 5 mM stock in DMSO). For washing out compounds, cultures were treated for 1 h with antibiotic, then 1 ml was pelleted, washed once in medium without antibiotic, and placed on an agarose pad without antibiotic.

As in particular during depletions a mix of live and dead cells accumulate over time, we counterstained these cultures with propidium iodide and only considered MreB fluorescence of cells that were non-fluorescent (=alive) for propidium iodide staining.

Epifluorescence microscope

Images of the vancomycin staining were acquired on a Nikon Eclipse TE2000-U microscope with X-cite 120 illumination system connected to a Hamamatsu digital camera model ORCA-ER. For the fluorescence image, an exposure time of 2 sec was used.

Spinning disk confocal microscope

Images in Fig. 2 were acquired on a Nikon TE2000 microscope equipped with a Yokogawa CSU-10 spinning disk and a perfect focus system. A plan Apo1.4 100x objective and an Andor Ixon DU897-E camera were used. To prevent phototoxicity, low laser illumination and short exposure times (150–300 ms) were used.

TIRF microscope

All other images were acquired on a Nikon N-STORM microscope equipped with an Andor Ixon 897 Ultra.Images were acquired using a 488 or 561 nm laser and a 100X 1.45 NA lambda objective, with 1 sec exposure time.

Image analysis

All images were analyzed using Fiji[48]. The plugin Multiple Kymograph (written by J. Rietdorf and A. Seitz) was used to create kymographs along 1 pixel wide lines. Kymographs were created at 4 locations perpendicular to the long axis of a representative cell. Image manipulation was limited to changing brightness and contrast for better presentation in print. All analysis was performed using raw images, unless it was necessary to align the time series for xy drifting using the Stackreg plugin[49]. The surface plots were created using the Interactive 3D Surface Plot plugin (written by K.-U. Barthel), and fluorescence intensities were measured using the Plot Profile function. The intensity variance over time analysis was performed using Matlab with the algorithm designed for measuring temporal variance in swarming microcolonies (Böttcher, Elliott *et al*., in preparation). It compares intensity changes at each pixel from one frame to the next, thus reporting where there is a high variance in pixel intensity that is resolvable over time.

Adjusting TIRF angle and focal plane to distinguish membrane and cytoplasmic localization

For distinguishing membrane and cytoplasmic localization, suitable TIRF angles were adjusted using the membrane dye FM4-64 (2 μM in PBS). The interval between angles was kept constant, as was the interval between the focal planes.

Fluorescent D-amino acid (FDAA) staining

Strains were grown in at 37°C while shaking until reaching exponential growth phase. Cells were treated with 20 μM targocil for one hour at 37°C. Then 3 ml of the culture were centrifuged (2 min 8000 g) and resuspended in 400 μl pre-warmed CH or LB containing targocil, if applicable. After approximately 5 min, fluorescently labeled D-amino acids (HADA) were added to a final concentration of 2 mM and labeling occurred at 37°C while shaking for 2 min as indicated. Then cells were fixed by addition of cold ethanol to a final concentration of 70%. Cells were incubated on ice for at least 15 min, then washed 2 times

in PBS, and eventually resuspended in PBS. Imaging was done using TIRF microscopy. For HADA, images were acquired with a 500 ms exposure with excitation at 405 nm at 25–40% laser power without using an emission filter.

Staining with fluorescent vancomycin

BODIPY®-FL vancomycin (Molecular Probes) was dissolved in water to a final concentration of 1 mg/ml and mixed with an equal volume of non-labeled vancomycin of the same concentration. 0.5 µl of the vancomycin mix was added to 1 ml of an growing cell culture (LB), either untreated or after 1 h treatment with inhibitors as indicated, and incubated shaking at 37°C for 2 min. Then 1 ml of 70% ethanol was added and the samples were incubated on ice for 15 min for fixation. The cells were then washed 3 times in PBS, mounted on 1% agarose in PBS pads and immediately imaged using the GFP filter set with an exposure time of 2 sec on the epifluorescence microscope.

RNA extraction and microarray

Changes in the transcriptome upon targocil treatment were determined using RNA microarray analysis. Strain KS002 was grown in LB to an OD_{600} of 0.4, then the culture was split in 2 and 20 µM targocil was added to one sample and DMSO alone to the other. RNA was extracted after 30 min shaking at 37°C using the Quiagen RNeasy Mini Kit with a modified protocol as described previously[50]. Final analysis was performed on the average of experimental triplicates, including dye flip for each.

Growth experiments

Strains were grown in LB with or without the addition of inducer and antibiotics as indicated. For growth curves, overnight cultures were diluted to an OD_{600} of 0.1 in fresh medium (200 µl volume in 96-well plate) and incubated at 37°C while shaking. Growth was measured by determining the OD_{600} every 20 min using a Promega GloMax Multi plate reader, or a Molecular Devices VersaMax plate reader. Colony forming units (CFUs) were determined by plating dilutions of a growing culture during a depletion experiment or before, during, and after treatment with targocil. To wash out the compound, the cells were pelleted, washed once with medium and resuspended to the same density. Inhibition by targocil was tested by soaking a small filter disk with 10 µl targocil (5 mM stock in DMSO) and placing it on a plate where the strain of interest had been spread.

Immunoblot

To test stability of MreB-GFP after treatment with cell wall inhibitors, strain bEG275 (P_{spank} MreB-gfp spc) was grown in LB containing 0.2 mM IPTG at 37°C. When the culture reached exponential growth, 2 µg/ml vancomycin was added for one hour to one sample. The cells were pelleted with the same OD_{600} for all samples and resuspended in 100 mM Tris pH 7, 500 mM sucrose, 10 mM $MgSO_4$. The samples were mixed with loading buffer and run on a 10% acrylamide SDS gel. The proteins were blotted on a nitrocellulose membrane and an immunoblot was performed using commercially available anti-GFP antibodies (anti-GFP rabbit IgG fraction, horseradish peroxidase conjugate, Life technologies™).

Strain construction

Inducible MreB-GFP fusion proteins—The fusions used were *amyE*::P_{spac} *mreB-gfp spc* (Alex Meeske), *yvbJ*::P_{xyl} *mreB-gfp erm* (Garner et al., 2011) and *amyE*::P_{xyl} *mreB-gfp spc*[51]. To visualize MreB in a targocil-sensitive strain, an MreB-GFP construct was inserted into KS002[24]. To visualize MreB in a strain lacking WTAs, *amyE*::P_{xyl} *mreB-gfp (spc)*[51] was introduced into a *tagO* null mutant[19].

sfGFP-PBP2A fusion—Native sfGFP fusion to Pbp2A was constructed by isothermal assembly. The region upstream of *pbpA* was amplified from PY79 DNA using primers o17/o18, the *erm* cassette was amplified from pGL83 using oEG001/oEG002. sfGFP was amplified from pGLFP26 using o23/o24, and an N terminal portion of *pbpA* was amplified from PY79 DNA using primers o25/o26. These fragments were fused using isothermal assembly, resulting in sfGFP in front of *pbpA*, resulting in a N-terminal fusion protein under control of its native promoter at its native locus. This was transformed into PY79 to give bMD98. Genomic DNA from bMD98 was transformed into bGL34to give bGL99, after checking for erythromycin, kanamycin, and chloramphenicol resistance, and IPTG sensitivity.

TagF depletion strain—To construct a strain with *tagF* under control of an inducible promoter, *tagF* was amplified from PY79 DNA using primers oEG139/oEG141, *xylR* and *erm* were amplified from pRB038 using primers oEG140/oEG142. These fragments were joined by isothermal assembly into plasmid pKM84 (cut with BamHI/SpeI) to give plasmid pEG114 which was linearized and then transformed into *B. subtilis* bKM424 (Rudner lab), giving strain bEG207 (spectinomycin sensitive, erythromycin resistant). Subsequently, the native *tagF* gene was deleted; for this, the up- and downstream regions of *tagF* was amplified using primers o9/o10, and o11/o12 respectively, and then fused with the chloramphenicol resistance marker cut from pKM074 (Rudner lab) by ligation. The whole fragment was re-amplified using o9/o12 and strain bEG207 was transformed with the linear PCR product, selection for chloramphenicol and erythromycin resistance and xylose dependence.

UppS depletion strain—This strain was constructed analogous to the TagF depletion strain. *uppS* was amplified using primers oEG136/oEG138 from py79 DNA, *xylR* and *erm* were amplified from pRB038 using primers oEG135/OEG137. All fragments were joined by isothermal assembly into plasmid pKM84 (cut with EcoRI/NheI) to give plasmid pEG119 which was then introduced into *B. subtilis* bKM424 (Rudner lab), resulting in strain bEG204 (spectinomycin sensitive, erythromycin resistant). To delete the endogenous *uppS* gene, up- and downstream flanking regions of *uppS* were amplified with primer pairs o1/o2 and o3/o4, respectively. These fragments were then combined by overlap PCR with a chloramphenicol cassette amplified with primers o15/o16 from pLI50 [52]. The linear construct was re-amplified with o1 and o4, and then introduced into bEG204. The resulting strain was tested for erythromycin and chloramphenicol resistance and xylose dependent growth.

Native promoter Mbl fusion—To verify that the observed phenotype was not due to overexpression, malfunction, or misregulation of the fusion protein we tested MreB and Mbl

fusions to GFP at the native locus under control of their native promoters. Native sfGFP fusion to the C-terminus of Mbl was constructed by isothermal assembly. The upstream part of *mbl* was amplified from PY79 DNA using primers o27/o28, sfGFP was amplified from pGLFP26 using o28/o29, and the spectinomycin resistance cassette was amplified from pGL80 using o31/o32. A downstream region of of *mbl* was amplified from PY79 DNA using primers o33/o34. These fragments were fused using isothermal assembly, resulting in sfGFP fused after *mbl* with a 15aa linker. This C-terminal fusion protein is under control of its native promoter at its native locus. This was transformed into PY79 to give bMD61. This strain showed equivalent doubling times to PY79.

Native promoter MreB fusion—To construct a strain with a C-terminal MreB-GFP fusion at the native locus under control of the native promoter we first placed the genes downstream of *mreB* under control of an inducible promoter. For this, we inserted an *erm* cassette and P_{xyl} between *mreB* and *mreC*, by the method of isothermal assembly. *erm* was PCR amplified using the primers o35 and o36 from plasmid pGL83. P_{xyl} and its repressor *xylR* were amplified from pGL26 using primers oMD72 and oMD73. Approximately 1200 bp upstream of *mreB* were amplified from genomic DNA from strain PY79 using primers oMD113 and oMD114. Approximately 1200 bp of *mreC*, for downstream homologous recombination, was amplified from genomic DNA from strain PY79 using primers oMD115 and oMD116. The four PCR products were assembled, PY79 was transformed with the assembled product, and erythromycin-resistant colonies were selected, yielding the xylose-dependent strain bMD88.

In this strain, *erm* and P_{xyl} were subsequently replaced with sfGFP including a 15 amino acid linker. For this, three PCR products were assembled by isothermal assembly. sfGFP was amplified with primers oMD90 and oMD91 from pGL-FP27; approximately 1200 bp upstream of *mreB*, were amplified from wt genomic DNA using primers mreBup2-fw and mreBup2-rev oMD134 and oMD89; and approximately 1200 bp within *mreC*, for downstream homologous recombination, were amplified from genomic DNA from strain PY79 using primers oMD92 and oMD 116. The three PCR products were then assembled, and bMD88 was transformed with the product. Selection on LB plates for growth in the absence of xylose without antibiotics resulted in strain bMD91. The genotype was confirmed by PCR and sequencing of the relevant region.

Stress response test strain—Pspac MreB-GFP was introduced into a strain carrying deletions of all seven known ECF sigma factors [38]. The deletion of all seven genes was tested by PCR using the primers specified by Asai et al.

MurG depletion strain—This strain was made by inserting an antibiotic cassette, P_{xyl}, and *xylR* in front of the *murG* coding region. Fragments for isothermal assembly were PCR-amplified using the following primer pairs: oPS01 and oPS02 for amplifying the fragment upstream of *murG* (including the *spoVE* terminator and *murG* promoter regions), and oPS03 and oPS04 for amplifying the *murG* coding region. oPS02 contained homologous DNA to the cat cassette, and oPS03 contained homologous DNA to the xylose cassette for isothermal assembly. The 4 pieces were assembled and the resulting fragment transformed into a wild-type strain.

Deposition of Microarray Data

The microarray data has been deposited on the GEO database under the accession number GSE54577.

Supplementary Material

Refer to Web version on PubMed Central for supplementary material.

Acknowledgments

This work was funded by NIH grants P01AI083214 and RO1GM076710 (to S.W.), NIH grant GM-047446 (to J.H.), NIH grant GM073831 (to D. Rudner for initial support of E.G.). E.G. was also supported by the Smith Family Award and a Searle Scholar Fellowship. K.S. gratefully acknowledges the DFG for a Research Fellowship. We thank Alex Meeske and David Rudner for strains bEG275 and bKM424, Kei Asai for strain BSU2007, and Patrick Stoddard for strain bPS01. We also thank Simon Ringgaard and Tom Bernhardt for critical reading of the manuscript. We are also grateful to Yves Brun for the fluorescent D-amino acids, and to Thomas Boettcher (HMS) and Hunter Elliott (Harvard Image and Data Analysis Core) for the temporal variance algorithm.

References

1. Garner EC, et al. Coupled, circumferential motions of the cell wall synthesis machinery and MreB filaments in *B. subtilis*. Science. 2011; 333:222–5. [PubMed: 21636745]
2. Domínguez-Escobar J, et al. Processive Movement of MreB-Associated Cell Wall Biosynthetic Complexes in Bacteria. Science. 2011; 333:225–228. [PubMed: 21636744]
3. Van Teeffelen S, et al. The bacterial actin MreB rotates, and rotation depends on cell-wall assembly. Proc Natl Acad Sci. 2011; 108:15822–15827. [PubMed: 21903929]
4. Kim SY, Gitai Z, Kinkhabwala A, Shapiro L, Moerner WE. Single molecules of the bacterial actin MreB undergo directed treadmilling motion in *Caulobacter crescentus*. Proc Natl Acad Sci U S A. 2006; 103:10929–34. [PubMed: 16829583]
5. Salje J, van den Ent F, de Boer P, Löwe J. Direct membrane binding by bacterial actin MreB. Mol Cell. 2011; 43:478–87. [PubMed: 21816350]
6. Reimold C, Defeu Soufo HJ, Dempwolff F, Graumann PL. Motion of variable length MreB filaments at the bacterial cell membrane influences cell morphology. Mol Biol Cell. 2013
7. Ingerson-Mahar M, Gitai Z. A growing family: the expanding universe of the bacterial cytoskeleton. FEMS Microbiol Rev. 2012; 36:256–267. [PubMed: 22092065]
8. Chastanet A, Carballido-López R. The actin-like MreB proteins in *Bacillus subtilis*: a new turn. Front Biosci (Scholar Ed). 2012:1582–1606.
9. Kawai Y, Asai K, Errington J. Partial functional redundancy of MreB isoforms, MreB, Mbl and MreBH, in cell morphogenesis of *Bacillus subtilis*. Mol Microbiol. 2009; 73:719–31. [PubMed: 19659933]
10. Schirner K, Errington J. The cell wall regulator σI specifically suppresses the lethal phenotype of *mbl* mutants in *Bacillus subtilis*. J Bacteriol. 2009; 191:1404–13. [PubMed: 19114499]
11. Wachi M, Matsuhashi M. Negative control of cell division by *mreB*, a gene that functions in determining the rod shape of *Escherichia coli* cells. J Bacteriol. 1989; 171:3123–3127. [PubMed: 2656641]
12. Typas A, Banzhaf M, Gross Ca, Vollmer W. From the regulation of peptidoglycan synthesis to bacterial growth and morphology. Nat Rev Microbiol. 2012; 10:123–136. [PubMed: 22203377]
13. Kawai Y, et al. A widespread family of bacterial cell wall assembly proteins. EMBO J. 2011; 30:4931–41. [PubMed: 21964069]
14. Kawai Y, Daniel RA, Errington J. Regulation of cell wall morphogenesis in *Bacillus subtilis* by recruitment of PBP1 to the MreB helix. Mol Microbiol. 2009; 71:1131–44. [PubMed: 19192185]

15. Varma A, Young KD. In Escherichia coli, MreB and FtsZ direct the synthesis of lateral cell wall via independent pathways that require PBP2. J Bacteriol. 2009; 191:3526–33. [PubMed: 19346310]
16. Carballido-López R, Formstone A. Shape determination in *Bacillus subtilis*. Curr Opin Microbiol. 2007; 10:611–6. [PubMed: 17981078]
17. Ursell TS, et al. Rod-like bacterial shape is maintained by feedback between cell curvature and cytoskeletal localization. Proc Natl Acad Sci U S A. 2014; 111:E1025–E1034. [PubMed: 24550515]
18. Brown S, Santa Maria JP, Walker S. Wall teichoic acids of Gram-positive bacteria. Annu Rev Microbiol. 2013; 67:313–36. [PubMed: 24024634]
19. D'Elia MA, Millar KE, Beveridge TJ, Brown ED. Wall teichoic acid polymers are dispensable for cell viability in *Bacillus subtilis*. J Bacteriol. 2006; 188:8313–6. [PubMed: 17012386]
20. D'Elia MA, et al. Probing teichoic acid genetics with bioactive molecules reveals new interactions among diverse processes in bacterial cell wall biogenesis. Chem Biol. 2009; 16:548–56. [PubMed: 19477419]
21. Formstone A, et al. Localization and interactions of teichoic acid synthetic enzymes in *Bacillus subtilis*. J Bacteriol. 2008; 190:1812–21. [PubMed: 18156271]
22. Swoboda JG, et al. Discovery of a small molecule that blocks wall teichoic acid biosynthesis in *Staphylococcus aureus*. ACS Chem Biol. 2009; 4:875–883. [PubMed: 19689117]
23. Lee K, Campbell J, Swoboda JG, Cuny GD, Walker S. Development of improved inhibitors of wall teichoic acid biosynthesis with potent activity against *Staphylococcus aureus*. Bioorg Med Chem Lett. 2010; 20:1767–70. [PubMed: 20138521]
24. Schirner K, Stone LK, Walker S. ABC transporters required for export of wall teichoic acids do not discriminate between different main chain polymers. ACS Chem Biol. 2011; 6:407–412. [PubMed: 21280653]
25. Afonso Lages MC, Beilharz K, Morales Angeles D, Veening JW, Scheffers DJ. The localization of key *Bacillus subtilis* penicillin binding proteins during cell growth is determined by substrate availability. Environ Microbiol. 2013; 15:3272–3281. [PubMed: 23895585]
26. Kuru E, et al. In Situ probing of newly synthesized peptidoglycan in live bacteria with fluorescent D-amino acids. Angew Chem Int Ed Engl. 2012; 51:12519–12523. [PubMed: 23055266]
27. Siegrist MS, et al. D-amino acid chemical reporters reveal peptidoglycan dynamics of an intracellular pathogen. ACS Chem Biol. 2013; 8:500–5. [PubMed: 23240806]
28. Ganchev DN, Hasper HE, Breukink E, de Kruijff B. Size and orientation of the lipid II headgroup as revealed by AFM imaging. Biochemistry. 2006; 45:6195–202. [PubMed: 16681392]
29. Strahl H, Bürmann F, Hamoen LW. The actin homologue MreB organizes the bacterial cell membrane. Nat Commun. 2014; 5:3442. [PubMed: 24603761]
30. Soldo B, Lazarevic V, Karamata D. *tagO* is involved in the synthesis of all anionic cell-wall polymers in *Bacillus subtilis* 168. Microbiology. 2002; 148:2079–87. [PubMed: 12101296]
31. Merrifield CJ, Feldman ME, Wan L, Almers W. Imaging actin and dynamin recruitment during invagination of single clathrin-coated pits. Nat Cell Biol. 2002; 4:691–8. [PubMed: 12198492]
32. Eiamphungporn W, Helmann JD. The *Bacillus subtilis* σM regulon and its contribution to cell envelope stress responses. Mol Microbiol. 2008; 67:830–48. [PubMed: 18179421]
33. Thackray PD, Moir A. SigM, an extracytoplasmic function sigma factor of *Bacillus subtilis*, is activated in response to cell wall antibiotics, ethanol, heat, acid, and superoxide stress. J Bacteriol. 2003; 185:3491–3498. [PubMed: 12775685]
34. Inoue H, Suzuki D, Asai K. A putative bactoprenol glycosyltransferase, CsbB, in *Bacillus subtilis* activates SigM in the absence of co-transcribed YfhO. Biochem Biophys Res Commun. 2013; 436:6–11. [PubMed: 23632331]
35. Lee YH, Helmann JD. Reducing the level of undecaprenyl pyrophosphate synthase has complex effects on susceptibility to cell wall antibiotics. Antimicrob Agents Chemother. 2013; 57:4267–4275.
36. Mascher T, Margulis NG, Wang T, Ye RW, Helmann JD. Cell wall stress responses in *Bacillus subtilis*: the regulatory network of the bacitracin stimulon. Mol Microbiol. 2003; 50:1591–1604. [PubMed: 14651641]

37. Cao M, Helmann JD. Regulation of the *Bacillus subtilis bcrC* Bacitracin Resistance Gene by Two Extracytoplasmic Function σ Factors. J Bacteriol. 2002; 184:6123–6129. [PubMed: 12399481]
38. Asai K, Ishiwata K, Matsuzaki K, Sadaie Y. A viable *Bacillus subtilis* strain without functional extracytoplasmic function sigma genes. J Bacteriol. 2008; 190:2633–6. [PubMed: 18223082]
39. Janas T, Chojnacki T, Swiezewska E. The effect of undecaprenol on bilayer lipid membranes. Acta Biochim Pol. 1994; 41:351–358. [PubMed: 7856407]
40. Delley, Pa; Hall, MN. Cell wall stress depolarizes cell growth via hyperactivation of RHO1. J Cell Biol. 1999; 147:163–74. [PubMed: 10508863]
41. Anderson JS, Matsuhashi M, Haskin MA, Strominger JL. Biosynthesis of the Peptidoglycan of Bacterial Cell Walls: II. Phospholipid carriers in the reaction sequence. J Biol Chem. 1967; 242:3180–3190. [PubMed: 6027793]
42. Tipper DJ, Strominger JL. Biosynthesis of the peptidoglycan of bacterial cell walls. XII Inhibition of cross-linking by penicillins and cephalosporins: studies in *Staphylococcus aureus in vivo*. J Biol Chem. 1968; 243:3169–3179. [PubMed: 5653196]
43. Lara B, Mengin-Lecreulx D, Ayala Ja, van Heijenoort J. Peptidoglycan precursor pools associated with MraY and FtsW deficiencies or antibiotic treatments. FEMS Microbiol Lett. 2005; 250:195–200. [PubMed: 16099113]
44. Brandish PE, et al. Modes of action of tunicamycin, liposidomycin B, and mureidomycin A: inhibition of phospho-N-acetylmuramyl-pentapeptide translocase from *Escherichia coli*. Antimicrob Agents Chemother. 1996; 40:1640–1644. [PubMed: 8807054]
45. Kahan FM, Kahan JS, Cassidy PJ, Kropp H. The mechanism of action of fosfomycin (phosponomycin). Ann N Y Acad Sci. 1974; 235:364–386. [PubMed: 4605290]
46. Carballido-López R, et al. Actin Homolog MreBH Governs Cell Morphogenesis by Localization of the Cell Wall Hydrolase LytE. Dev Cell. 2006; 11:399–409. [PubMed: 16950129]
47. Bach JN, Bramkamp M. Flotillins functionally organize the bacterial membrane. Mol Microbiol. 2013; 88:1205–1217. [PubMed: 23651456]
48. Schindelin J, et al. Fiji: an open-source platform for biological-image analysis. Nat Methods. 2012; 9:676–82. [PubMed: 22743772]
49. Thévenaz P, Ruttimann UE, Unser M. A pyramid approach to subpixel registration based on intensity. IEEE Trans Image Process. 1998; 7:27–41. [PubMed: 18267377]
50. Hachmann AB, et al. Reduction in membrane phosphatidylglycerol content leads to daptomycin resistance in *Bacillus subtilis*. Antimicrob Agents Chemother. 2011; 55:4326–37. [PubMed: 21709092]
51. Defeu Soufo HJ, Graumann PL. Dynamic movement of actin-like proteins within bacterial cells. EMBO Rep. 2004; 5:789–94. [PubMed: 15272301]
52. Lee CY, Buranen SL, Ye ZH. Construction of single-copy integration vectors for *Staphylococcus aureus*. Gene. 1991; 103:101–5. [PubMed: 1652539]

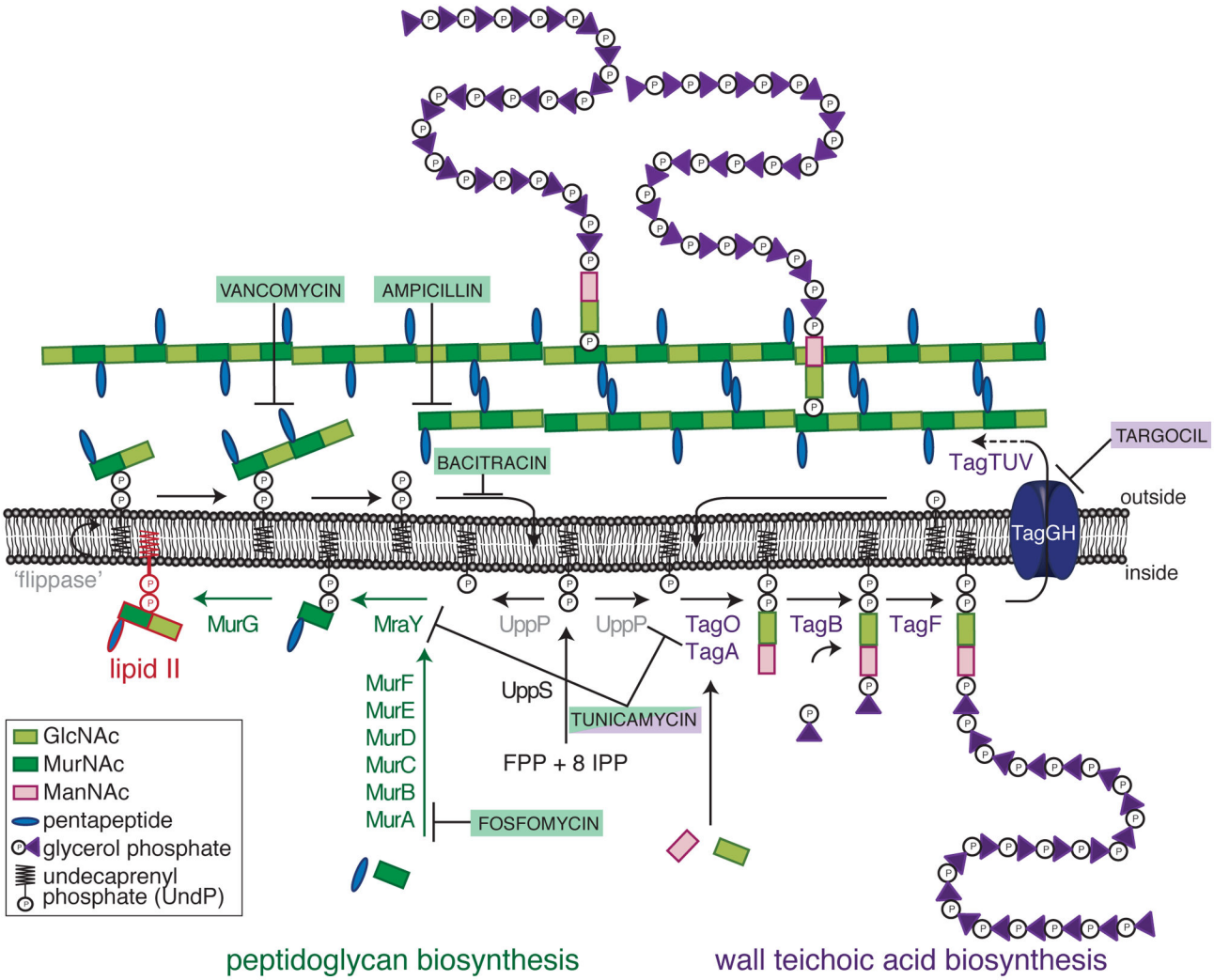

Fig. 1. Schematic of the cell wall synthetic pathways in *B. subtilis*

The peptidoglycan synthesis pathway is shown on the left in green, and the wall teichoic acid pathway is on the right in purple. Both pathways use the carrier lipid undecaprenol phosphate (UndP). Boxed writing indicates inhibitors and their targets. GlcNAc = N-acetyl glucosamine; MurNAc = N-acetyl muramic acid; ManNAc = N-acetyl mannosamine; FPP = farnesyl pyrophosphate; IPP = isoprene phosphate.

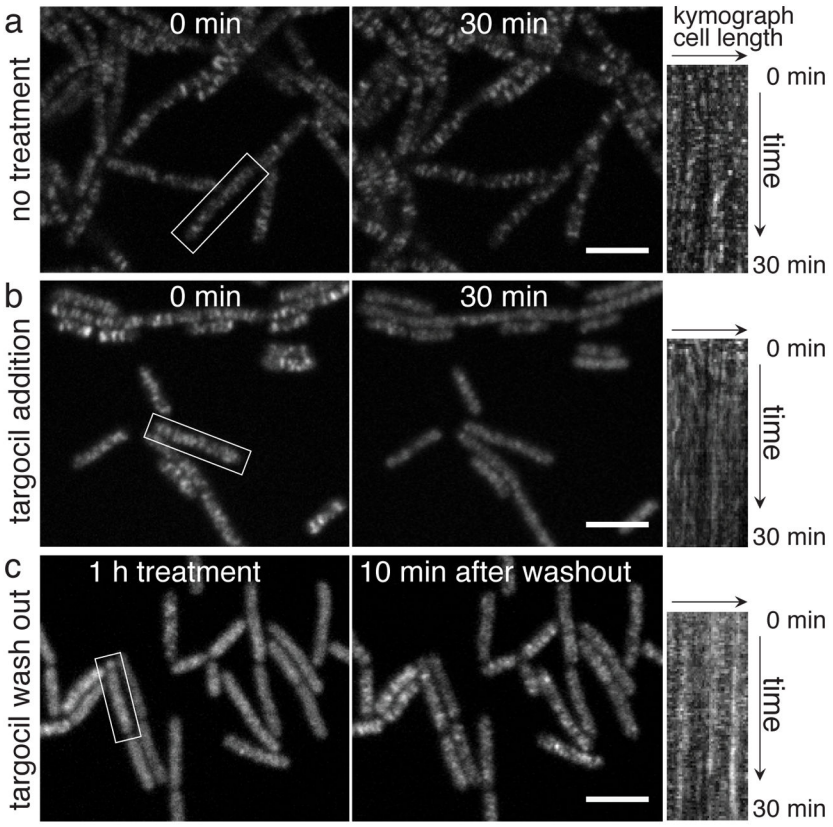

Fig. 2. Inhibition of WTA export with targocil leads to dissolving of the MreB cytoskeleton

a. Time lapse of a targocil-sensitive *B. subtilis* strain expressing MreB-GFP (strain EG133) without any treatment. Images were acquired every 20 sec for 30 min on a spinning disk confocal microscope. The kymograph on the right represents MreB signal along the length of the marked cell over time. b. Time lapse of a targocil-sensitive *B. subtilis* strain expressing MreB-GFP (strain EG133) during targocil treatment. Images were taken every 20 sec, and targocil was added onto the agarose pad after frame 3. Shown are snapshots before treatment (0 min) and half an hour after adding targocil (30 min). The kymograph on the right represents MreB signal along the length of the marked cell over time. c. Time lapse of the same strain after treating the cells for one hour with targocil and then imaging them after washing out the compound, relieving the block of the WTA exporter. Shown are snapshots of the treated cells and 10 min after washing out the compound. The kymographs represent MreB dynamics along the length of the boxed cell over time. Scale bars: 5 μm. See also Supplementary Movie 1.

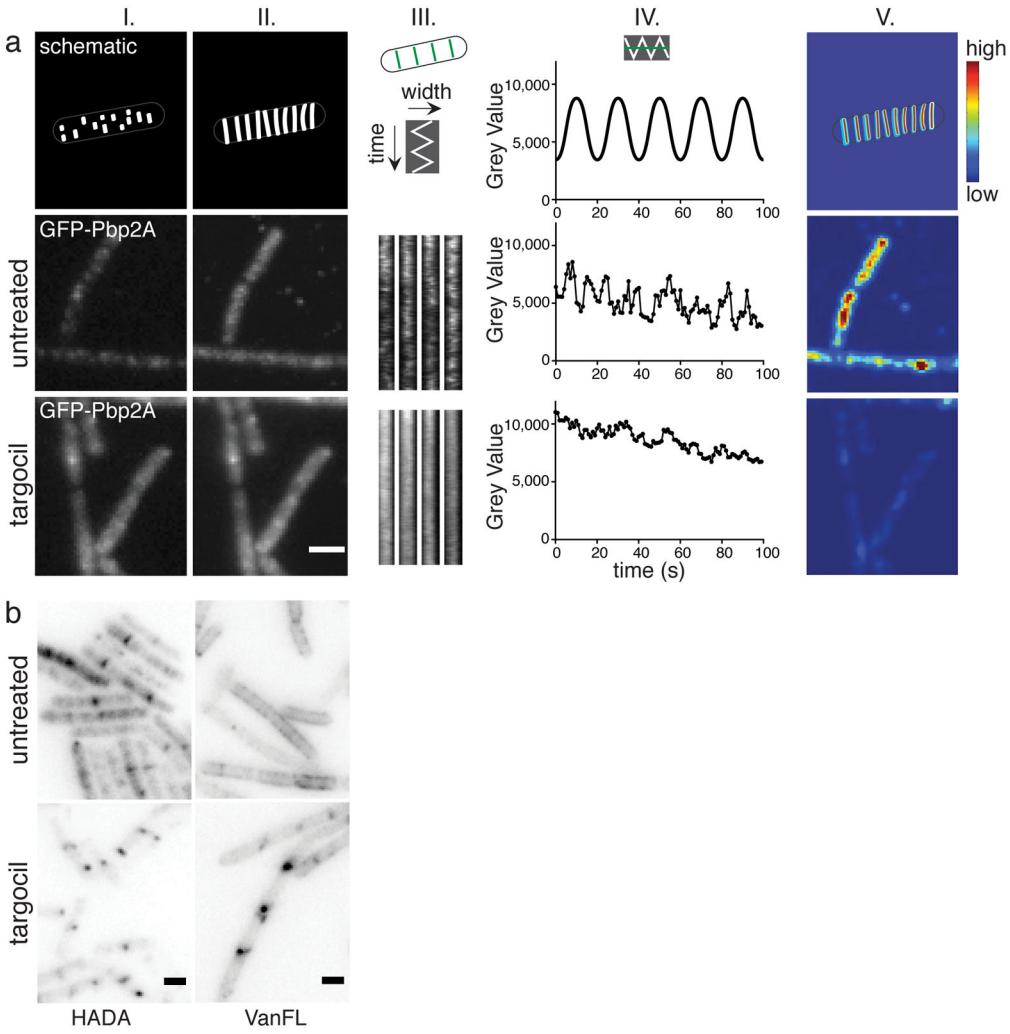

Fig. 3. PG synthesis is mislocalized after WTA inhibition

a. The top row shows a schematic showing the analysis of an experiment, as explained in the text. The two rows below show the localization of Pbp2A-GFP (strain bGL99) in untreated cells and in cells treated with targocil for 1 h. In panels of column I snapshots of a time lapse are shown. In column II panels, the maximum intensities of all images are superimposed. Panels in column III show kymographs taken perpendicular to the long axis of a cell. Column IV panels show the measurement of fluorescence intensity over the middle of a kymograph. Column V panels show a plot of the variance of fluorescence intensity over time, with red indicating regions of high intensity variances and blue areas indicating regions of low intensity variances. All time lapse series shown here were acquired over 100 sec in 1 sec frames with streaming acquisition. b. Labeling of nascent PG with the fluorescent D-amino acid HADA or fluorescent vancomycin in untreated and targocil treated cells (strain KS002). Exponentially growing cultures were pulsed with HADA for 2 min before fixing, then imaged using a TIRF microscope. Similarly, exponentially growing cultures were pulsed for 2 min with a mix of fluorescently labeled and unlabeled

vancomycin, then fixed, and subsequently imaged on an epifluorescence microscope. Scale bars: 2 μm. See also Supplementary Movie 4.

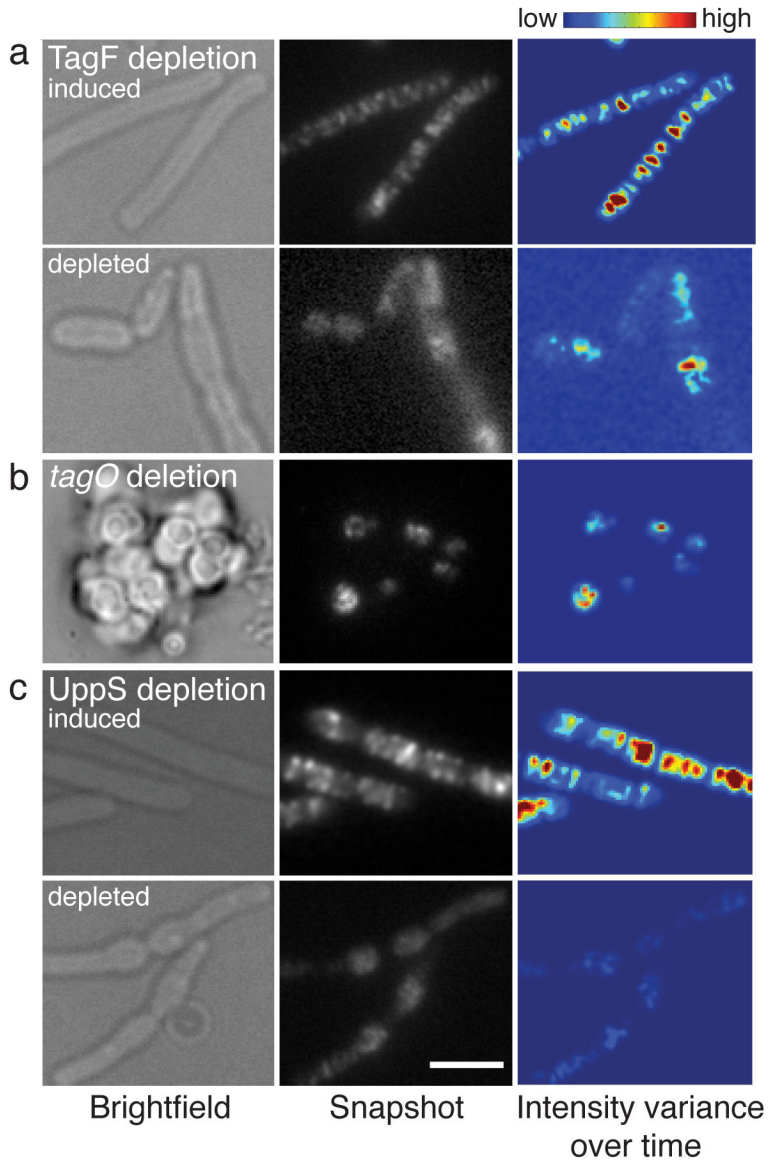

Fig. 4. Availability of the carrier lipid, but not cell surface WTA, is required for MreB filament formation

a. MreB-GFP in a TagF-depletion strain (bGL23) before (induced) and 2 h after removal of the inducer (depleted). Depletion of TagF leads to the buildup of lipid-linked short WTA precursors, resulting in depletion of the carrier lipid. b. MreB-GFP in a WTA-less *tagO* deletion strain (EG203). c. MreB-GFP in a strain with the UndP synthase UppS under control of an inducible promoter (bGL24); the top row shows cells grown in the presence of inducer (induced), the bottom row cells 4 h after removal of the inducer (depleted). When UppS is absent, the carrier lipid cannot be made and consequently neither WTA nor PG can be synthesized. All time lapses were taken by imaging every 10 sec for 5 min on a TIRF microscope, and shown are a brightfield image, a snapshot of the time lapse, and the intensity variance. Scale bar: 5 μm. See also Supplementary movies 5–7.

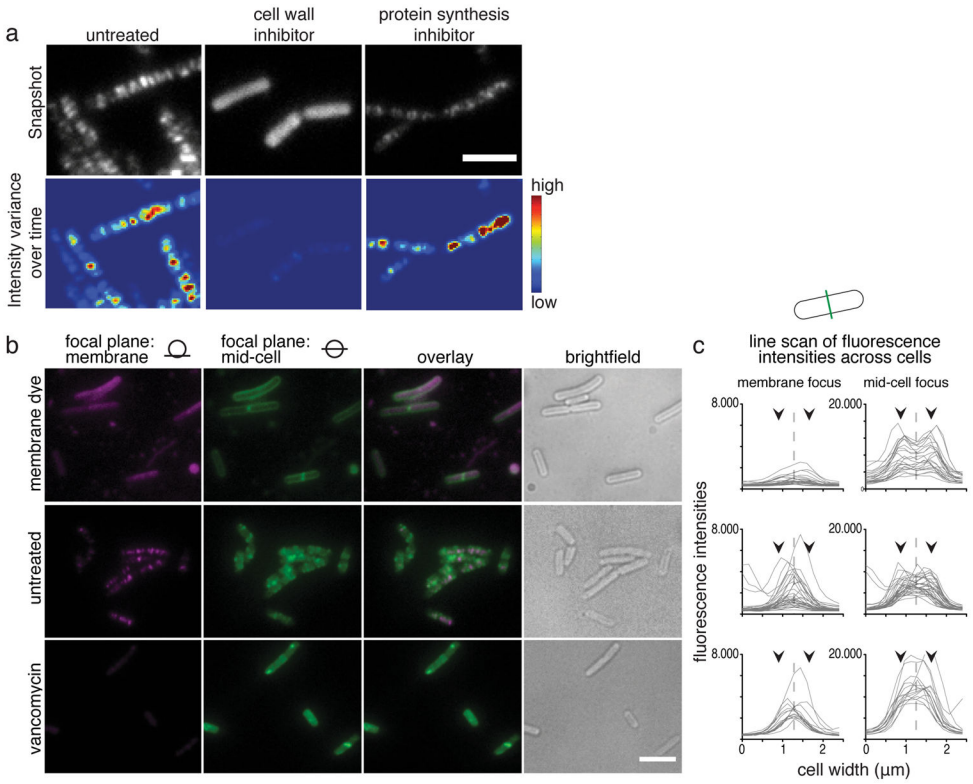

Fig. 5. Prolonged treatment with cell wall inhibitors leads to dissolution of MreB into the cytoplasm

a. Time-lapse analysis of MreB-GFP (EG275, BRB687) in untreated cells (left), cells treated with a cell wall inhibitor (here vancomycin, middle), and cells treated with a protein synthesis inhibitor (here tetracycline, right). Shown here is a snapshot and the temporal variance analysis of a time lapse series over 5 min with a 10 sec frame rate. Further inhibitors of each class were tested and the results including the full analysis are shown in Supplementary Figure 4. b. Images acquired with distinct illumination angles and focal planes of cells stained with a membrane dye (top), of MreB-GFP in untreated cells (middle) and of MreB-GFP in cells treated with vancomycin for 1 h. Shown are images of the membrane focal plane, a mid-cell focal plane, an overlay of these two, and a brighfield image, with the scale bar representing 5 μm. c. Measurements of fluorescence intensities across the width of each cell in the field both of membrane and of mid-cell focus images. The dotted line indicates half of the cell width, and the arrows point to the positions of the cell membrane.

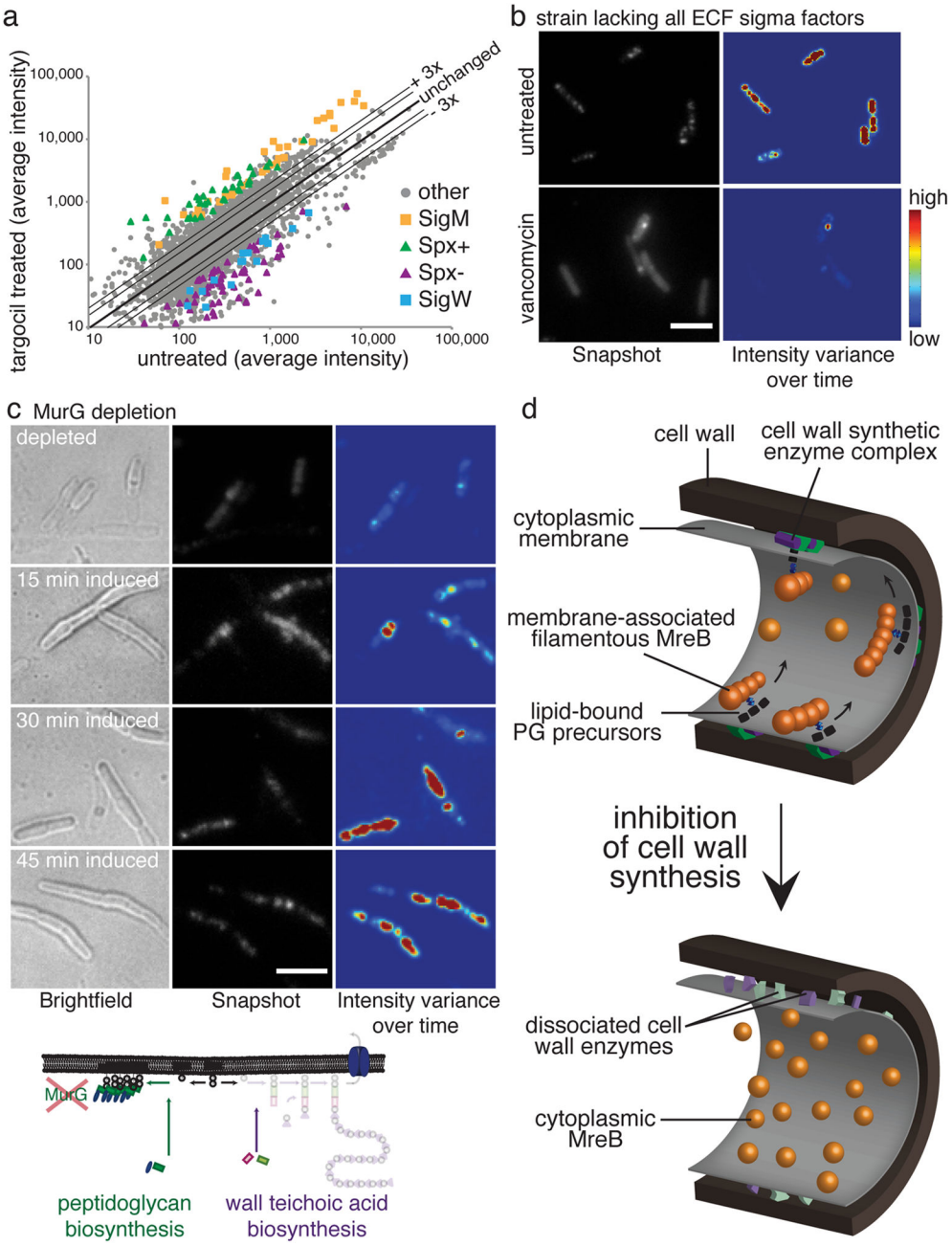

Fig. 6. Presence of lipid II is required for MreB filament formation and motion

a. Transcriptional profile of 30 min targocil treatment (strain KS002), presented as a plot of average intensities of on a microarray (3 biological replicates, including dye flip of each). Members of the main regulons activated during targocil treatment are colored as indicated. b. MreB-GFP in a strain without ECF sigma factors (bGL125), with and without vancomycin treatment for 1 h. Shown are snapshots and temporal variance analysis. Images were acquired every 10 sec for 5 min on a TIRF microscope. c. MreB-GFP in a MurG depletion strain (bJE16) 4 h after removing inducer, and then 15, 30, and 45 min after adding inducer again. Images were acquired on a TIRF microscope every 10 sec for 5 min.

Scale bars represent 5 μm. d. Model of interactions between MreB and lipid-linked PG precursors, regulating MreB membrane association and filament formation.